Title

Emotion-related impulsivity is related to orbitofrontal cortical sulcation.

Authors

Hastings Iii, William
Willbrand, Ethan
Kelly, Joseph
et al.

Publication Date

2024-12-01

DOI

10.1016/j.cortex.2024.08.009

Peer reviewed

HHS Public Access

Author manuscript

Cortex. Author manuscript; available in PMC 2024 December 28.

Published in final edited form as:

Cortex. 2024 December ; 181: 140–154. doi:10.1016/j.cortex.2024.08.009.

Emotion-related impulsivity is related to orbitofrontal cortical sulcation

William L. Hastings III[a], **Ethan H. Willbrand**[b], **Joseph P. Kelly**[c], **Sydney T. Washington**[d], **Phyllis Tameilau**[a], **Reyansh N. Sathishkumar**[e], **Samira A. Maboudian**[f,g], **Benjamin J. Parker**[f,g], **Matthew V. Elliott**[a], **Sheri L. Johnson**[a], **Kevin S. Weiner**[a,f,g,*]

[a]Department of Psychology, University of California, Berkeley, Berkeley, CA, USA

[b]Medical Scientist Training Program, School of Medicine and Public Health, University of Wisconsin–Madison, Madison, WI, USA

[c]Department of Psychiatry and Behavioral Sciences, Feinberg School of Medicine, Northwestern University, IL USA

[d]Department of Psychology, California State University, Fullerton, Fullerton, CA, USA

[e]Cognitive Science Program, University of California, Berkeley, Berkeley, CA, USA

[f]Helen Wills Neuroscience Institute, University of California, Berkeley, Berkeley, CA, USA

[g]Department of Neuroscience, University of California, Berkeley, Berkeley, CA, USA

Abstract

Background: Emotion-related impulsivity (ERI) describes the trait-like tendency toward poor self-control when experiencing strong emotions. ERI has been shown to be elevated across psychiatric disorders and predictive of the onset and worsening of psychiatric syndromes.

[*]*Corresponding author*. Department of Psychology, University of California, Berkeley, Berkeley, CA, USA. kweiner@berkeley.edu (K.S. Weiner).

CRediT authorship contribution statement

William L. Hastings: Writing – review & editing, Writing – original draft, Visualization, Software, Methodology, Investigation, Formal analysis, Data curation, Conceptualization, Project administration. **Ethan H. Willbrand:** Writing – review & editing, Writing – original draft, Validation, Supervision, Software, Project administration, Methodology, Investigation, Formal analysis, Data curation, Conceptualization, Visualization. **Joseph P. Kelly:** Formal analysis, Investigation, Software, Visualization, Writing – original draft, Writing – review & editing, Data curation, Methodology, Validation. **Sydney T. Washington:** Data curation, Formal analysis, Investigation, Writing – review & editing. **Phyllis Tameilau:** Data curation, Formal analysis, Investigation, Writing – review & editing. **Reyansh N. Sathishkumar:** Data curation, Visualization, Writing – review & editing. **Samira A. Maboudian:** Formal analysis, Investigation, Validation, Writing – review & editing. **Benjamin J. Parker:** Formal analysis, Investigation, Validation, Writing – review & editing. **Matthew V. Elliott:** Writing – review & editing, Writing – original draft, Resources, Data curation, Conceptualization. **Sheri L. Johnson:** Writing – review & editing, Writing – original draft, Supervision, Resources, Funding acquisition, Data curation, Conceptualization, Project administration. **Kevin S. Weiner:** Writing – review & editing, Writing – original draft, Visualization, Validation, Supervision, Software, Project administration, Methodology, Investigation, Funding acquisition, Data curation, Conceptualization.

Declaration of Competing Interest

All authors report no biomedical financial interest or potential conflicts of interest.

Open practices

The study in this article has earned Open Data badge for transparent practices. The data are available at: https://github.com/cnl-berkeley/stable_projects/tree/main/ERI_OFC_Sulcation and https://nda.nih.gov/edit_collection.html?id=2455.

Supplementary data

Supplementary data to this article can be found online at https://doi.org/10.1016/j.cortex.2024.08.009.

Recent work has correlated ERI scores with the region-level neuroanatomical properties of the orbitofrontal cortex (OFC), but not posteromedial cortex (PMC). Informed by a growing body of research indicating that examining the morphology of specific cortical folds (sulci) can produce unique insights into behavioral outcomes, the present study modeled the association between ERI and the morphology of sulci within OFC and PMC, which is a finer scale than previously conducted.

Methods: Analyses were conducted in a transdiagnostic sample of 118 adult individuals with a broad range of psychiatric syndromes. First, we manually defined over 4,000 sulci across 236 cerebral hemispheres. Second, we implemented a model-based LASSO regression to relate OFC sulcal morphology to ERI. Third, we tested whether effects were specific to OFC sulci, sulcal depth, and ERI (as compared to PMC sulci, sulcal gray matter thickness, and non-emotion-related impulsivity).

Results: The LASSO regression revealed bilateral associations of ERI with the depths of eight OFC sulci. These effects were strongest for OFC sulci, sulcal depth, and ERI in comparison to PMC sulci, sulcal gray matter thickness, and non-emotion-related impulsivity. In addition, we identified a new transverse component of the olfactory sulcus in every hemisphere that is dissociable from the longitudinal component based on anatomical features and correlation with behavior, which could serve as a new transdiagnostic biomarker.

Conclusions: The results of this data-driven investigation provide greater neuroanatomical and neurodevelopmental specificity on how OFC is related to ERI. As such, findings link neuroanatomical characteristics to a trait that is highly predictive of psychopathology.

Keywords

Emotion; MRI; Neuroanatomy; Orbitofrontal cortex; Psychopathology; Self-control; Transdiagnostic

1. Introduction

Understanding the neuroanatomical basis of psychopathology is a major interest of cognitive and clinical neuroscience. Determining the neural correlates underlying emotion-related impulsivity (ERI; Carver & Johnson, 2018; Pearlstein, Johnson, Modavi, Peckham, & Carver, 2019); is particularly important as ERI is increasingly recognized as a shared trait across many psychological disorders (Pearlstein et al., 2019; Pearson, Combs, Zapolski, & Smith, 2012; Riley, Combs, Jordan, & Smith, 2015) and is predictive of numerous internalizing and externalizing syndromes (Berg, Latzman, Bliwise, & Lilienfeld, 2015; Johnson, Carver, & Joormann, 2013, 2017). Despite the well-established predictive power of ERI, neurobiological correlates of ERI are still largely unknown (Johnson, Elliott, & Carver, 2020).

In the present work, our main region of interest was the orbitofrontal cortex (OFC) given that previous functional and structural imaging work has suggested a link between ERI, psychopathology more broadly, and OFC morphology (Elliott, Esmail, Weiner, & Johnson, 2023; Hiser & Koenigs, 2018; Nakamura, Nestor, & Shenton, 2020; Owens et al., 2020). Specifically motivating the present study, previous work identified (i) a qualitative

link between the pattern of cortical indentations, or sulci, in OFC and clinical outcomes (Nakamura et al., 2020) and (ii) a quantitative link between the local gyrification of OFC and ERI (Elliott et al., 2023). Here, we also considered the posteromedial cortex (PMC) as a control region for three reasons. First, PMC is generally implicated in psychopathology and impulsive behavior (Foster et al., 2023; Hazlett et al., 2005; Leech & Sharp, 2014; Miglin et al., 2019; Zhao et al., 2017). Second, prior work on the neuroanatomy of ERI did not identify a relationship between PMC and ERI using exploratory quantitative analyses on local gyrification at the group level (Elliott et al., 2023). Third, our group recently clarified the sulcal organization of PMC (Willbrand, Maboudian, et al., 2023; Willbrand, Parker, et al., 2022), allowing for a more precise, individual-level exploration of the previously-identified group-level null finding (Elliott et al., 2023). Altogether, while a growing body of work has identified quantitative relationships between sulcal morphology in different parts of the cerebral cortex with multiple behavioral and psychiatric outcomes (Brun et al., 2016; Garrison et al., 2015; Maboudian et al., 2024; Parker et al., 2023; Ramos Benitez et al., 2024; Voorhies, Miller, Yao, Bunge, & Weiner, 2021; Willbrand, Ferrer, Bunge, & Weiner, 2023; Willbrand, Tsai, Gagnant, & Weiner, 2023; Yao, Voorhies, Miller, Bunge, & Weiner, 2022), it is presently unknown if there is an anatomo-cognitive link between the morphology of individual sulci and ERI in OFC and PMC.

To begin to fill this gap in knowledge, we examined the relationship between ERI and OFC and PMC sulcal morphology in a transdiagnostic sample of 118 individuals with a broad range of internalizing and externalizing syndromes following a “precision imaging” approach (Gratton et al., 2020). To do so, we defined putative primary, secondary, and tertiary sulci in each individual hemisphere, resulting in over 4,000 manually defined sulci across the sample. We then implemented a model-based LASSO regression to relate OFC and PMC sulcal morphology to ERI, and subsequently tested whether effects were specific to ERI (as compared to non-emotion-related impulsivity) and OFC (as compared to PMC). We focused on sulcal depth as it is one of the main morphological features differentiating putative primary (deepest), secondary, and tertiary (shallowest) sulci from one another and recent research identifies a link between sulcal depth and cognition (Brun et al., 2016; Voorhies et al., 2021; Willbrand, Tsai, et al., 2023; Yao et al., 2022). To our knowledge, this is the first study to examine the relationship between ERI and sulci identified in each individual hemisphere that also includes putative tertiary sulci, which have been largely overlooked and are considerably variable across hemispheres (Amiez et al., 2019, 2023; Garrison et al., 2015; Lopez-Persem, Verhagen, Amiez, Petrides, & Sallet, 2019; Maboudian et al., 2024; Miller, D’Esposito, & Weiner, 2021; Voorhies et al., 2021; Willbrand, Maboudian, et al., 2023; Willbrand, Parker, et al., 2022; Willbrand, Tsai, et al., 2023; Willbrand, Voorhies, Yao, Weiner, & Bunge, 2022; Yao et al., 2022).

2. Materials and methods

2.1. Dataset

We report how we determined our sample size, all data exclusions (if any), all inclusion/exclusion criteria, whether inclusion/exclusion criteria were established prior to data analysis, all manipulations, and all measures in the study.

2.1.1. Participants—This study aims to primarily assess the behavioral relevance of orbitofrontal (OFC) and posteromedial (PMC) sulcal morphology across a transdiagnostic sample of individuals with a wide range of internalizing and externalizing syndromes. The sample consisted of 118 participants (ages 18–55 years old; 67% female, 28% male, and 5% non-binary; participant demographic details are provided in Supplementary Table 1). This sample and associated data (MRI scans, and behavioral data; detailed below) were also used in our previous work assessing the relationship between local gyrification and ERI (Elliott et al., 2023); however, it is worth noting that the neuroanatomical scales are completely different [automatically defined anatomical large-scale regions in Elliott et al. (2023) versus the level of fine-scale individual sulci in the present work). Further, the actual data extracted and analyzed here are completely new (i.e., morphological features of individual sulci in individual participants; detailed below). Therefore, the present work is distinguishable from this prior work and, importantly, aims to build upon the previous work by evaluating the relationship between OFC morphology and ERI at a far finer scale than previously assessed.

Most participants demonstrated substantial impairment due to mental health symptoms, as indicated by receipt of disability, mental health services or by scores greater than 5 on the Sheehan Disability Scale (Leon, Olfson, Portera, Farber, & Sheehan, 1997); to sample a fuller range of impairment, though, 17 individuals with Sheehan Disability scores less than or equal to 5 were included. The UC Berkeley Committee for the Protection of Human Subjects approved the parent study supported by the National Institutes of Health (NIH; Grant No. R01MH110477 [to S.L.J.]. Researchers recruited participants through flyers, online advertising, and referrals from clinicians and excluded individuals with current alcohol or substance abuse disorders, a history of bipolar disorder or primary psychosis (as assessed by the SCID for DSM-5; participant diagnosis details are included in Supplementary Table 1), or daily use of marijuana or sedating medications (participant medication use is detailed in Supplementary Table 2), as well as those with lifetime head trauma resulting in loss of consciousness for five or more minutes, low cognitive abilities (Orientation Memory Concentration Test (Katzman et al., 1983) score of less than 7), MRI safety contraindications, neurological disorders, or inability to complete cognitive measures due to intellectual or language impairment. After researchers gave informed consent, participants completed diagnostic, behavioral, and neuroimaging sessions (Elliott et al., 2023). Before the neuroimaging session, participants completed urine toxicology screening.

2.1.2. Behavioral measures—The mental health-related impairment of the participants was assessed using the Sheehan Disability Scale (Leon et al., 1997). The Orientation Memory Concentration Test was used (Katzman et al., 1983) to further identify any potential cognitive deficits. ERI was assessed using the well-validated Three Factor Impulsivity Index, which contains three factor-analytically derived subscales with robust internal consistency (Carver, Johnson, Joormann, Kim, & Nam, 2011; Johnson, Tharp, Peckham, Carver, & Haase, 2017). The first factor, Feelings Trigger Action (FTA), covers the propensity to act or speak rashly while experiencing high (positively or negatively valenced) emotions. This factor is composed of three facets: the Negative Urgency Scale, Positive Urgency Measure, and Reflexive Reaction to Feelings Scale (Carver et al., 2011; Whiteside

& Lynam, 2001). The second factor, Pervasive Influence of Feelings (PIF), comprises three facets that assess cognitive and motivational reactions, mostly towards negative emotions: Generalization, Sadness Paralysis, and Emotions Color Worldview (Carver, Voie, Kuhl, & Ganellen, 1988, 2011). The third factor, Lack of Follow Through (LFT), covers impulsivity without reference to emotion, including Lack of Perseverance and Distractibility (Carver et al., 2011; Whiteside & Lynam, 2001).

The response format for all items consists of ratings on a scale of 1 “I agree a lot” to 5 “I disagree a lot”; higher scores indicate higher severity. Across previous studies, PIF and FTA, the two forms of ERI, exhibit a more substantial correlation with psychopathology measures compared to LFT (Auerbach, Stewart, & Johnson, 2017; Johnson et al., 2013, 2017). Given this, we hypothesized that OFC sulcal morphology would be correlated with these two factors, and we included analyses of LFT as a control measure. ERI measures were unrelated to age, gender, and current medication status (Supplementary Table 3).

2.1.3. Magnetic resonance imaging data—

Individuals participated in a brain imaging scan using a 3 T Siemens TIM Trio magnetic resonance imaging (MRI) scanner with a 32-channel receiver head coil. The scanner acquired sagittal T1-weighted structural images with a standard 6.1 min magnetization-prepared rapid gradient-echo sequence (MPRAGE) utilizing the following parameters: Repetition Time = 1900 msec, Echo Time = 2.89 msec, Field of View = 256 mm, Voxel size = 1 mm isotropic voxels, PAT Mode = GRAPPA, and PE = 2. Before the scan, researchers reminded participants to remain as still as possible, and presented participants with a blank screen during the scan(Elliott et al., 2023).

2.2. Analysis pipeline

2.2.1. Manual definition of orbitofrontal sulci—

The structural T1-weighted scans underwent processing through FreeSurfer (version 6.0.0; https://surfer.nmr.mgh.harvard.edu (Dale, Fischl, & Sereno, 1999; Fischl & Dale, 2000). We employed the built-in function recon-all to transform 2D high-resolution anatomical images into 3D pial and inflated cortical reconstructions. The curvature metric within FreeSurfer was used to differentiate between sulcal and gyral components (Dale et al., 1999; Fischl & Dale, 2000; Wandell, Chial, & Backus, 2000).

W.L.H. and E.H.W. manually identified OFC sulci in each hemisphere (N = 118; 236 hemispheres) using FreeSurfer’s tksurfer tools and guided by the latest definition of OFC sulci (Petrides, 2019). Every label was then validated by a neuroanatomist with expertise in OFC (K.S.W.) prior to any morphological analyses. The OFC sulci of interest in the present study were the: (1) olfactory sulcus (olfs), (2) transverse olfactory sulcus (tolfs), (3) transverse orbital sulcus (tos), (4) anterior section of the medial orbital sulcus (mos-a), (5) posterior section of the medial orbital sulcus (mos-p), (6) anterior section of the lateral orbital sulcus (los-a), (7) posterior section of the lateral orbital sulcus (los-p), (8) intermediate orbital sulcus (ios), (9) posterior orbital sulcus (pos), and (10) sulcus fragmentosis (sf). Prior research has shown that the olfs, tos, mos-a, mos-p, los-a, and los-p are present in all individuals, whereas the ios, pos, and sf are more variably present

(Chiavaras & Petrides, 2000). In the present work, we could identify the horizontal tolfs as distinct from the longitudinal olfs in every hemisphere. Fig. 1a provides a visual representation of left and right hemispheres for reference. OFC sulcal definitions in all participants are provided in Supplementary Fig. 1.

2.2.2. Identifying "Types" of OFC sulcogyral patterns—We categorized each hemisphere's sulcogyral organization based on a classification system developed by Chiavaras and Petrides (2000) and refined by Chakirova et al. (2010); Fig. 1b i–iv). Type I, the most prevalent sulcal pattern across samples (Nakamura et al., 2020), displays a discontinuity between the anterior and posterior components of the medial orbital sulci, while the anterior and posterior components of the lateral orbital sulcus are continuous. Type II demonstrates continuity between the anterior and posterior components in both the medial and lateral orbital sulci. Type III shows discontinuity between the anterior and posterior components of both the medial and lateral orbital sulci. Type IV, the least common and typically excluded from analysis, exhibits discontinuity in the anterior and posterior components of the lateral orbital sulci, but not the medial orbital sulci. We also assessed the number of variable putative tertiary sulci–sulci with an incidence rate that varies from zero to up to four components across individuals–in each hemisphere. Similar to the labeling process, each pattern underwent assessment and validation before any further analyses were performed.

As it is becoming more commonly performed in the field (Borst et al., 2016; Cachia et al., 2016; Eichert, Watkins, Mars, & Petrides, 2021; Roell et al., 2021), to define sulci in the present study, we used each participant's 3D native cortical surface mesh (inflated and pial FreeSurfer cortical surface reconstructions) as this 1) preserves the participant's native sulcal morphology, 2) automatically parses the gyral versus sulcal portions of the cortex, and 3) allows for the viewing of buried gyri/*plis de passage*. Importantly, the OFC pattern types were also originally documented on postmortem brains (Chiavaras & Petrides, 2000), and in vivo sulcal patterning visualized via FreeSurfer cortical surface reconstructions accurately reflects that of postmortem brains (Willbrand, Parker, et al., 2022; Willbrand, Tsai, et al., 2023). Altogether, this facilitates the discernment of sulcal discontinuity that is not subject to bias based on the number of 2D slides examined. There was strong inter-rater agreement in OFC type classification (Cohen's κ [95% CI] = .94 [.91–.98]).

2.2.3. Manual definition of posteromedial sulci—In the present study, we also considered 8–13 sulci within posteromedial cortex (PMC) that were recently identified and comprehensively described in our prior work (Willbrand, Maboudian, et al., 2023; Willbrand, Parker, et al., 2022). We considered three consistent sulci that bound PMC: parietooccipital sulcus (POS), marginal ramus of the cingulate sulcus (MCGS), and splenial sulcus (spls). We also considered the more variable border sulcus: premarginal branch of the cingulate sulcus (pmcgs). We considered four consistent sulci within the precuneal cortex (PrC; the superior subregion of PMC): dorsal precuneal limiting sulcus (prculs-d) and three precuneal sulci (posterior: prcus-p, intermediate: prcus-i, anterior: prcus-a). There was one variable PrC sulcus we also considered: ventral precuneal limiting sulcus (prculs-v). Within the posterior cingulate cortex (PCC; the inferior subregion of PMC), we identified

between one and four sulci. The inframarginal sulcus (ifrms) is consistently present in every human hemisphere. Anterior to the ifrms, there is a variably present indentation termed the posterior intracingulate sulcus (icgs-p). Posterior to the ifrms, we could identify up to two variable sulci: the dorsal (sspls-d) and ventral (sspls-v) subsplenial sulci. W.L.H. and S.T.W. manually identified PMC sulci in a subset of participants who had OFC sulci identified ($N = 102$; 204 hemispheres) using FreeSurfer's tksurfer tools. Every label was then validated by four neuroanatomists with expertise in PMC prior to any morphological analyses (E.H.W., J.P.K., S.A.M., K.S.W.). The incidence rates of PMC sulci in this sample are detailed in the Supplementary Results. The incidence rates of the five variable PMC sulci are shown in Supplementary Table 4. PMC sulcal definitions in all participants are provided in Supplementary Fig. 2.

2.2.4. Extracting morphological features—After sulci were defined, depth (according to FreeSurfer values; Dale et al., 1999), cortical thickness (in millimeters; Fischl & Dale, 2000), and surface area (in square millimeters; Fischl, Sereno, Tootell, & Dale, 1999) were calculated using an established analysis pipeline and the mris_anatomical_stats function in FreeSurfer (Miller, Voorhies, Lurie, D'Esposito, & Weiner, 2021; Voorhies et al., 2021). These metrics commonly discriminate sulcal types from one another. For example, primary sulci are the deepest with the largest surface area, while putative tertiary sulci are the shallowest with the smallest surface area (Armstrong, Schleicher, Omran, Curtis, & Zilles, 1995; Chi, Dooling, & Gilles, 1977; Welker, 1990). The latter are particularly intriguing when considering neurodevelopmental disorders as they emerge last in gestation in association cortices and continue to develop after birth. Depth values, as computed by FreeSurfer, depend on the distance of a vertex from the "mid-surface," with the mean displacements around this "mid-surface" being zero. This usually results in gyri having negative values, while sulci have positive values. However, due to the shallowness and variability in the depths of putative tertiary sulci, some mean depth values can be less than zero. To account for variations in brain size among individuals and hemispheres, we employed normalized sulcal depth, consistent with previous studies (Maboudian et al., 2024; Voorhies et al., 2021; Willbrand, Ferrer, et al., 2023; Willbrand, Tsai, et al., 2023; Yao et al., 2022). Cortical thickness and sulcal depth of all OFC sulci are shown in Supplementary Fig. 3.

2.3. Data analysis

2.3.1. Categorical measurements—We first considered the relationship between ERI and two categorical measures describing OFC sulci. The first was the Type of OFC sulcogyral pattern (incidence in Supplementary Fig. 4a). The second was the total number of variable (putative tertiary) OFC sulci (incidence in Supplementary Fig. 4b–d). For these two categorical measures, we conducted a Type III Analysis of Variance (ANOVA) to compare incidence rates for each ERI factor. When relevant, post hoc *t*-tests were applied and *P*-values were corrected with the Tukey multiplicity adjustment (Schaarschmidt, Ritz, & Hothorn, 2022; Searle, Speed, & Milliken, 1980).

2.3.2. Continuous measurements—Building upon our prior work (Maboudian et al., 2024; Voorhies et al., 2021; Willbrand, Ferrer, et al., 2023; Willbrand, Tsai, et al., 2023;

Yao et al., 2022), to analyze continuous morphological sulcal–behavior relationships, we leveraged a pre-existing pipeline that tests for a relationship between sulcal morphology and ERI via the following data-driven approach.

1. L1 regularization (least absolute shrinkage and selection operator, LASSO, regression): A LASSO regression is well suited to this situation as it facilitates model selection and increases the generalizability and preventing overfitting (particularly in cases where there are $10 < x < 25$ events per variable) of a model by providing a sparse solution that reduces coefficient values and decreases variance in the model without increasing bias (Heinze, Wallisch, & Dunkler, 2018). Specifically, LASSO performs L1 regularization by applying a penalty, or shrinking parameter (alpha value), to the absolute magnitude of the coefficients such that low coefficients are set to zero and eliminated from the model. Thus, LASSO facilitates data-driven variable selection, leading to a parsimonious, yet comprehensive, model where only the sulci most associated with the outcome measure remain as predictors in the model. As a result, this data-driven method improves the interpretability and prediction accuracy of a model, while simultaneously safeguarding against overfitting and maximizing generalizability (Ghojogh & Crowley, 2019; Heinze et al., 2018).

2. Cross-validation: Our LASSO regression models were tuned and evaluated using cross-validation, a within-sample method for improving the generalizability of a model that is standard practice in machine learning (Ghojogh & Crowley, 2019; Poldrack, Huckins, & Varoquaux, 2020; Vabalas, Gowen, Poliakoff, & Casson, 2019). Cross-validation creates a series of within-sample train/test splits that allows for every data point to be used for both training and testing. In the present study, we used leave-one-participant-out cross-validation (LOOCV), in which the model is successively fit to every data point except one and then tested on the left-out data point. We first conducted a grid search with LOOCV to select the value of the shrinking parameter (a) that minimized mean squared error (MSE) of the model (Heinze et al., 2018). We then used a second LOOCV to calculate cross-validated R^2 and MSE values and thereby evaluate the model. In a supplementary analysis, we ran the same LASSO pipeline again but with fully nested cross-validation, a procedure in which parameter tuning and feature selection are performed separately for each cross-validation fold. Fully nested cross-validation is the most rigorous, least biased method for within-sample development of predictive models (Poldrack et al., 2020; Vabalas et al., 2019). This supplementary analysis confirmed results from the original analysis (Supplementary Materials).

3. Permutation Testing: In all analyses, we submitted statistical results (MSE, Spearman's rho) from the LASSO-selected models to random permutation testing. Permutation testing is a robust non-parametric alternative to standard parametric significance tests because it does not rely on distributional assumptions such as normality, homogeneity of variance, or random sampling. It is a powerful tool for evaluating test statistics from the modest sample sizes characteristic of neuroimaging studies. Using 5,000 permutations of the dataset,

in which behavioral scores were randomly shuffled, we generated empirical null distributions of MSE and Spearman's rho, which we compared with the observed MSE and Spearman's rho values from the selected model. Permutation testing yields exact *p*-values (P^*_n = 5,000).

The LASSO approach requires that all sulci are present in each hemisphere. As such, to balance the number of sulci and number of participants in the models, we excluded the pos and ios as they were the most variable (Supplementary Fig. 4b and c), resulting in eight sulci being submitted to the model: (1) olfs, (2) tolfs, (3) tos, (4) mos-a, (5) mos-p, (6) los-a, (7) los-p, (8) sf. In total, morphological data from the 109 left hemispheres and 102 right hemispheres that contained these eight sulci were included in the models testing for a relationship between OFC sulcal morphology with the two emotionally driven ERI factors (PIF and FTA) in each hemisphere separately. Any LASSO-selected models (determined via the three-fold approach described previously) were then compared to two alternative models to assess specificity. The first model acted as a surface-based measurement control (cortical thickness) and the second served as a behavioral control (Lack of Follow Through). We assessed how our model performed relative to the control models by measuring the difference of their Akaike Information Criterion [AIC (Akaike, 1998);]. We also assessed the regional specificity of any ERI factor that was significantly related to OFC sulcal depth by re-implementing the LASSO approach with the depths of PMC sulci instead (Supplementary Materials). Given the null relationship between ERI and age (Supplementary Table 3) and the inconsistent relationship between sulcal morphology and age (OFC: Supplementary Table 5; PMC: Supplementary Table 6), age was not included in any of the models. No part of the study procedures or analyses were pre-registered prior to the research being conducted.

3. Results

3.1. Overview of orbitofrontal sulcal incidence and sulcogyral patterning

We were able to identify nine sulci that have been previously identified and explored, six of which were identifiable within the orbitofrontal cortex (OFC) in every hemisphere: 1–2) the posterior and anterior portions of the lateral orbital sulcus (los-a, los-p), 3–4) the anterior and posterior portions of the medial orbital sulcus (mos-a, mos-p), 5) the transverse orbital sulcus (tos), and 6) the olfactory sulcus (olfs). Three additional sulci could be defined in some, but not all, hemispheres across participants: (1) the intermediate orbital sulcus (ios), (2) the posterior orbital sulcus (pos), and (3) sulcus fragmentosis (sf). Additionally, these sulci varied in the number of observed components, ranging from zero to as many as four components (Fig. 1a; Supplementary Fig. 4b–d).

3.2. The transverse olfactory sulcus is morphologically distinct from the olfactory sulcus

For the first time (to our knowledge), we were also able to identify the transverse olfactory sulcus (tolfs) in every hemisphere examined (Fig. 1a; Supplementary Fig. 1). Though many neuroanatomists throughout history have acknowledged a "hook" at the posterior extent of the olfactory sulcus (additional details are provided in the Supplementary Materials and Supplementary Figs. 5–6), the present study is the first (to our knowledge) to define and

label this component separately. Comparing cortical thickness and depth between the olfs and tolfs revealed that the latter is significantly deeper and thicker (Tukey's $P < .0001$ for all comparisons) than the former (Fig. 2), providing empirical evidence that the tolfs is morphologically distinct from the olfs.

3.3. OFC sulcogyral types in the present study are consistent with a previous meta-analysis

OFC sulcogyral patterns varied (Fig. 1b; Supplementary Fig. 4a) with comparable incidence rates reported first by Chiavaras and Petrides (2000) and by subsequent studies (reviewed by Nakamura et al., 2020). To directly compare our incidence rates to those previously reported, we performed a meta-analysis comparing the incidence rates in the present study to studies reporting OFC sulcogyral patterns in neurotypical controls (12 studies, 710 total participants; Fig. 3a), and clinical samples (13 studies, 869 total participants; Fig. 3b). The clinical samples comprised individuals with first episode psychosis, ultra-high risk of psychosis, schizophrenia, schizotypal, and autism spectrum disorder, all of which have reported sulcogyral incidence rates (Bartholomeusz et al., 2013; Chakirova et al., 2010; Chiavaras & Petrides, 2000; Lavoie et al., 2014; Li, Sescousse, Amiez, & Dreher, 2015; Nakamura et al., 2007, 2008, 2020; Nishikawa et al., 2016; Rodrigues et al., 2015; Uehara-Aoyama et al., 2011; Watanabe et al., 2014; Whittle et al., 2014). The results of this meta-analysis showed that the OFC sulcogyral types in the present study are consistent with these previous studies (Fig. 3; Supplementary Table 1). Indeed, ANOVAs examining the effect of sulcogyral type on each factor of ERI revealed no significant effects across all comparisons (ps > .05).

We also assessed the relationship between the incidence of the variable OFC sulci (pos, ios, and sf; Fig. 1a; Supplementary Fig. 4b–d) and ERI given (i) the relationship between sulcal incidence, behavior, and psychopathology more generally (Cachia et al., 2021) and (ii) the incidence of the variable OFC sulci and psychopathology specifically (Nakamura et al., 2020). ANOVAs examining the effect of the number of variable sulci on each factor of ERI revealed no significant effects across all comparisons (ps > .05).

3.4. The depths of a subset of OFC sulci are related to ERI

We implemented data-driven LASSO regression models using the sulcal depths of the eight most consistent OFC sulci (tos, tolfs, sf, olfs, mosp, mosa, losp, losa) in the left and right hemispheres separately to predict each emotionally related ERI factor: (i) Feelings Trigger Action (FTA) and (ii) Pervasive Influence of Feelings (PIF; Materials and Methods). From these models, the OFC sulcal depth in the left and right hemispheres independently predicted FTA, but not PIF. More specifically, between the two hemispheres, the LASSO regression selected the depths of eight OFC sulci that were associated with FTA at the optimum alpha threshold of the model (right hemisphere: $\alpha = .043$, MSE = .496; left hemisphere: $\alpha = .032$, MSE = .500; Fig.4). In the right hemisphere, the depth of the olfactory sulcus ($\beta = -.07$), as well as the posterior component of both the lateral ($\beta = .16$) and medial ($\beta = -.08$) orbital sulci were associated with, FTA ($R^2_{CV} = .06$, $MSE_{CV} = .487$, $P^*_{n = 5,000} = .019$; Fig. 4a). In the left hemisphere, the depth of the sulcus fragmentosis ($\beta = -.12$), olfactory sulcus ($\beta = -.13$), anterior ($\beta = .12$) and posterior (β

= .05) components of the medial orbital sulcus, as well as the anterior component of the lateral orbital sulcus (β = −.06) were associated with FTA (R^2_{CV} = .07, MSE_{CV} = .490, $P^*_{n = 5,000}$ = .006; Fig. 4b). In both hemispheres, Spearman correlations between predicted and measured FTA scores showed that the LASSO-selected models significantly predicted individual differences in FTA scores (right hemisphere: Spearman's rho = .27, $P^*_{n = 5,000}$ = .002; left hemisphere: Spearman's rho = .24, $P^*_{n = 5,000}$ = .005). We also implemented a maximally rigorous model-selection process using fully nested cross-validation to further ensure the generalizability of our results (Materials and Methods), which confirmed results from the original model (Supplementary Results; Supplementary Fig. 7). Conversely, using the same approach to predict PIF scores, we found no relationship between OFC sulcal depth and PIF. No sulci were selected by the LASSO regression in either hemisphere (right hemisphere: α = .126,MSE = .566;lefthemisphere: α = .141, MSE = .603), which resulted in intercept-only models (R^2s = .0).

Next, we assessed the specificity of the LASSO-selected models associating OFC sulcal depth to FTA in both hemispheres (right hemisphere: FTA ~ olfs + mos-p + los-p; left hemisphere: FTA ~ sf + olfs + mos-a + mos-p + los-a) by leveraging the Akaike Information Criterion (AIC; Akaike, 1998) to compare them to control models for both behavior and morphology (Materials and Methods). When comparing two models, a ΔAIC greater than 2 indicates an interpretable difference between models, while a ΔAIC greater than 10 indicates a substantial difference, with the lower AIC value indicating the preferred model (Burnham & Anderson, 2004; Wagenmakers & Farrell, 2004). With regards to behavior, we compared the AIC of LASSO-selected models associating OFC sulcal depth to FTA to models associating the sulcal depth of these same OFC sulci in each hemisphere to a non-emotional impulsivity metric: Lack of Follow Through (LFT; Materials and Methods). The difference in AIC between the LASSO-selected models for sulcal depth and FTA and LFT indicates that the predictive value of OFC sulcal depth is substantially stronger for FTA than it is for the non-emotional counterpart (right hemisphere: $\Delta AIC_{LFT\text{-}FTA}$ = 27.6; left hemisphere: $\Delta AIC_{LFT\text{-}FTA}$ = 29.0). With regards to morphology, we compared the AIC of the LASSO-selected models associating OFC sulcal depth to FTA to models associating the cortical thickness of these same sulci in each hemisphere to FTA (Materials and Methods). The sulcal depth model was preferred over the cortical thickness model in both hemispheres (right hemisphere: $\Delta AIC_{Thickness\text{-}Depth}$ = 6.7; left hemisphere: $\Delta AIC_{Thickness\text{-}Depth}$ = 16.2). We also tested for regional specificity of the relationship between sulcal depth and FTA by implementing the same data-driven LASSO regression approach on the depths of sulci within posteromedial cortex (PMC), which identified that the depths of PMC sulci were less associated and predictive of FTA than the depths of OFC sulci (Supplementary Results; Supplementary Fig. 8).

Finally, we tested the impact of defining the tolfs separately from the olfs on our models. To do so, we generated a separate model which did not differentiate the transverse portion from the main branch of the olfs. This "olfactory complex" had decreased β-values compared to the olfs in the original model (Supplementary Fig. 9). This provides additional empirical evidence that the tolfs should be defined separately from the olfs.

4. Discussion

In the present study, we examined the relationship between OFC sulcal morphology and ERI in a transdiagnostic clinical sample. To do so, we manually defined over 4,000 sulci in individual participants and implemented a model-based approach, which revealed bilateral associations of ERI with the depths of eight OFC sulci. These effects were strongest for ERI, sulcal depth, and OFC sulci as compared to non-emotion-related impulsivity, sulcal cortical thickness, and PMC sulci. In addition, we identified a new transverse component of the olfactory sulcus in every hemisphere that is dissociable from the longitudinal component based on anatomical features and correlation with behavior. The results of this data-driven investigation provide greater neuroanatomical and neurodevelopmental specificity on how OFC is related to ERI than previous studies, as well as link neuroanatomical characteristics to a trait that is highly predictive of psychopathology. Together, our findings provide an important step in clarifying the neuroanatomical correlates of ERI, a foundation that can be built upon in future studies. In the sections below, we discuss these results in the context of previous findings, as well as consider goals for future work.

In previous work, Elliott et al. (2023) established a neuroanatomical link between OFC and ERI. Using a continuous global surface-based morphological measurement, the authors identified a link between ERI and the local gyrification of OFC. Building on that work which used an automated algorithm to define the perimeter of a large OFC region of interest (ROI), here, we improved the spatial scale of our measurements from one large OFC ROI to manually defined OFC sulci in each individual hemisphere (in line with what has been referred to as a “precision imaging” approach (Gratton et al., 2020). As such, the present findings identify precise neuroanatomical sulcal landmarks that are related to ERI and complement the previous findings. For example, Elliott et al. (2023) identified a stronger relationship between FTA and the OFC in the left hemisphere. Our model-based approach also identified a hemispheric difference in which the depths of five sulci in the left hemisphere and only three in the right hemisphere were related to ERI that provide two key insights. First, the model identified only two sulci (olfs and mos-p) in both the right and left hemispheres, indicating bilateral sulcal landmarks related to ERI for the first time. To remind the reader, it is important to note that this olfs definition does not include the tolfs; when including the tolfs in the definition of an “olfs complex,” the model fit decreased (Supplementary Fig. 9). As prior findings show that the depth of the olfs is typically decreased in patients with or at risk of developing schizophrenia (Takahashi et al., 2013, 2014, 2019; Turetsky, Crutchley, Walker, Gur, & Moberg, 2009), our findings indicate that the olfs, but not the tolfs, could be driving those effects. This dissociation can be examined in future research. Second, the model identifies both large, primary sulci and small, putative tertiary sulci such as the sf (Fig. 4). Thus, it is not just primary, secondary, or tertiary sulci that are driving the effects previously identified; instead, it is a sulcal landscape of eight OFC sulci between the two hemispheres that are related to ERI.

There are also differences between the present and previous findings (Elliott et al., 2023) indicating that the neuroanatomical correlates of FTA and PIF may operate on different spatial scales. For example, there was no significant relationship of PIF with sulcal depth, whereas Elliott et al. (2023) found that PIF correlated bilaterally to the local gyrification

of OFC. As such, PIF may function at a coarser level in OFC (broad, non-sulcal-specific folding) while FTA appears to be localized to specific structures. In a similar vein, and more broadly, our present findings also indicate that ERI as a construct relates more to fine-grained, continuous features of the cortex that coarser, categorical measures like sulcal incidence cannot properly capture. For example, the incidence rate of variable sulci was not significantly related to impulsivity levels, despite prior work indicating that the number of variable sulci present in clinical populations relates to psychopathology severity (Nakamura et al., 2020). Taken together, the combination of the present and previous findings underscores how psychopathology manifests in the OFC on multiple scales, some of which appear to overlap with impulsivity–as observed in global and local continuous measurement scales with respect to ERI–while others do not.

By focusing on sulci within OFC, we have improved the spatial scale of the neuroanatomical underpinnings of ERI. Nevertheless, it may be tempting to also conclude that these structures are the most important neuroanatomical link to ERI (i.e., a more localized "modular" view). We emphasize that the neuroanatomical underpinnings of ERI likely include many more neuroanatomical structures across spatial scales and that our present findings are the next step in uncovering the infrastructure of a complex neural network underlying ERI that is presently unknown (Zachlod, Palomero-Gallagher, Dickscheid, & Amunts, 2023). Indeed, previous findings relating sulcal morphology to cognition in different populations discuss the relationship between sulcal morphology and network connectivity with an emphasis on white matter architecture (Fornito et al., 2006; Garrison et al., 2015; Le Provost et al., 2003; Miller, Voorhies, et al., 2021; Voorhies et al., 2021; Yao et al., 2022; Yücel et al., 2002). Further, although empirical investigation on the functional importance of OFC sulci is still in early stages (e.g., Li et al., 2015; Troiani, Dougherty, Michael, & Olson, 2016, 2020), to begin exploring how the functional neuroanatomy of these sulci may relate to ERI, we leveraged the Neurosynth meta-analysis software (Yarkoni, Poldrack, Nichols, Van Essen, & Wager, 2011) to compare the location of OFC sulci to the location of activation across dozens of fMRI studies for different search terms relating to both OFC (Rolls, 2004; Rolls, Cheng, & Feng, 2020) and FTA (Carver & Johnson, 2018; Pearlstein et al., 2019). This procedure revealed multiple putative correspondences (Supplementary Fig. 10). These relationships can be used in future research to explore the functional cortical infrastructure that could underlie why these sulci relate to ERI. Altogether, the present work identifies a local sulcal network in OFC bilaterally related to ERI that will serve as the foundation for identifying additional neuroanatomical, functional, and cognitive components of the complex multimodal network underlying ERI for decades to come.

Zooming out, the present results appear to further bridge parallel transdiagnostic literatures in psychiatry and neuroscience. For example, while ERI has been well-explored and accepted as a transdiagnostic phenotype in clinical literature (Carver, Johnson, & Timpano, 2017; Caspi & Moffitt, 2018; Smith, Atkinson, Davis, Riley, & Oltmanns, 2020), explorations of OFC anatomy and psychopathology appears to be less explored, with few studies testing for similarities across diagnostic boundaries (Cardenas et al., 2011; Drevets, 2007; Eckart et al., 2011; Patti & Troiani, 2018; Rogers & De Brito, 2016). To bridge between these parallel tracks, we recently proposed that ERI could serve as an

intermediate psychological phenotype that emerges from the development of OFC and leads to psychopathology (Elliott et al., 2023). Here, we extend this proposal to also include the emergence of neuroanatomical structures. That is, sulci emerge at different time points in gestation and a classic theory proposes that in a given cortical expanse, sulci that emerge later will be related to aspects of cognition that have a protracted development (Sanides, 1962, 1964). Consistent with this idea, Chi et al. (1977) observed that the posterior extent of the olfs–consistent with the location of the tolfs in the present study–emerged first (around 16 gestational weeks), while the more anterior longitudinal component emerged significantly later (around 25 gestational weeks; additional details are provided in the Supplementary Materials). The fact that our model identified the olfs, but not the tolfs, bilaterally suggests the intriguing possibility that the later emergence and development of the olfs, not the tolfs, could be related to ERI. Longitudinal research will be needed to test this hypothesis.

We are hopeful that the neuroanatomical and model-based approach implemented in the present study can support future work on ERI and generalize to other research domains that seek to integrate the transdiagnostic study of psychopathology at two crucial levels of analysis: psychiatry and neuroscience. To expedite this goal, tools are actively being developed to leverage deep learning algorithms as a guide to semi-automate the definition of neuroanatomical structures such as the small and variable putative tertiary sulci explored here (Borne, Rivière, Mancip, & Mangin, 2020; Lee, Willbrand, Parker, Bunge, & Weiner, 2024; Hao et al., 2020). Such tools will be sure to increase the sample size, which is a main limitation of the present study, as well as shed further light on the relationship between putative tertiary sulci and psychopathology. That is, despite Sanides' classic hypothesis (1962, 1964), tertiary sulci have been widely overlooked for methodological reasons (Miller, D'Esposito, & Weiner, 2021) and the broad fields of psychiatry and neuroscience know very little about their development, morphological changes across the lifespan, and if/how the development and changes across the lifespan relate to psychiatric outcomes. An important next step will be to include tertiary sulci in neuroanatomical investigations in different clinical populations, which could have implications for mental health treatment. For example, the depth of one of the smallest and shallowest sulci in OFC, the sf (Fig. 1a; Supplementary Fig. 3b), explained the most variance of all left hemisphere sulci identified by our model (Fig. 4). Lastly, considering that the structure and function of the prefrontal cortex (PFC) is related to impulsivity in patients with schizophrenia (Hoptman, Antonius, Mauro, Parker, & Javitt, 2014) and contains numerous tertiary sulci (Amiez et al., 2023; Miller, Voorhies, et al., 2021; Petrides, 2019; Voorhies et al., 2021; Willbrand et al., 2024; Willbrand, Ferrer, et al., 2023; Willbrand, Voorhies, et al., 2022; Yao et al., 2022), future work should also assess the relationship between PFC sulcal morphology and ERI.

5. Conclusion

The present study sought to directly extend recent work showing a relationship between the regional gyrification of OFC and ERI (Elliott et al., 2023) by providing greater neuroanatomical specificity through investigating if the morphology of specific sulci within OFC is related to ERI. A data-driven approach leveraging thousands of manually-defined sulci in over a hundred transdiagnostic adult participants identified a morphologically-,

cognitively-, and regionally-specific robust relationship between the depths of multiple OFC sulci and a distinct dimension of ERI: Feelings Trigger Action. To conclude, as OFC and ERI have both been responsive to existing treatments spanning cognitive behavioral therapy (Jensen et al., 2012; Johnson et al., 2020), cognitive training (Engvig et al., 2010; Miotto et al., 2006; Peckham & Johnson, 2018), and mindfulness (Deplus, Billieux, Scharff, & Philippot, 2016; Fox et al., 2014; Zeidan et al., 2015), the present findings suggest that future intervention studies targeting the sulci identified here may be promising for treating psychopathology transdiagnostically.

Supplementary Material

Refer to Web version on PubMed Central for supplementary material.

Acknowledgments

We thank W. Voorhies and J. Miller for developing the data analysis pipelines implemented in the present work, as well as K. Timpano, K. Modavi, A. Dev, M. Robison, J. Mostajabi, S. Esmail, and B. Weinberg for their help with recruitment and data collection. We also thank N. Angelides, H.Y. Tsai, M. Andrews, and J. Giffin for their help with magnetic resonance imaging data acquisition.

Funding

This work was supported by the National Institutes of Health R01 MH110447 (SLJ), the Brain and Behavior Research Foundation NARSAD 30738 (KSW), National Science Foundation CAREER 2042251 (KSW), the National Institutes of Health Medical Scientist Training Program T32 GM140935 (EHW), and the National Institutes of Health T32 NS047987 (JPK). The funding agencies did not have a role in the study design, data collection and analysis, decision to publish, or preparation of the manuscript.

REFERENCES

Akaike H (1998). A new look at the statistical model identification. In Parzen E, Tanabe K, & Kitagawa G (Eds.), Selected papers of Hirotugu Akaike (pp. 215–222). New York: Springer. 10.1007/978-1-4612-1694-0_16.

Amiez C, Sallet J, Giacometti C, Verstraete C, Gandaux C, Morel-Latour V, et al. (2023). A revised perspective on the evolution of the lateral frontal cortex in primates. Science Advances, 9(20), Article eadf9445. 10.1126/sciadv.adf9445 [PubMed: 37205762]

Amiez C, Sallet J, Hopkins WD, Meguerditchian A, Hadj-Bouziane F, Ben Hamed S, et al. (2019). Sulcal organization in the medial frontal cortex provides insights into primate brain evolution. Nature Communications, 10(1), 1–14. 10.1038/s41467-019-11347-x

Armstrong E, Schleicher A, Omran H, Curtis M, & Zilles K (1995). The ontogeny of human gyrification. Cerebral Cortex, 5(1), 56–63. 10.1093/cercor/5.1.56 [PubMed: 7719130]

Auerbach RP, Stewart JG, & Johnson SL (2017). Impulsivity and suicidality in adolescent inpatients. Journal of Abnormal Child Psychology, 45(1), 91–103. 10.1007/s10802-016-0146-8 [PubMed: 27025937]

Bartholomeusz CF, Whittle SL, Montague A, Ansell B, McGorry PD, Velakoulis D, et al. (2013). Sulcogyral patterns and morphological abnormalities of the orbitofrontal cortex in psychosis. Progress in Neuro-Psychopharmacology & Biological Psychiatry, 44, 168–177. 10.1016/j.pnpbp.2013.02.010 [PubMed: 23485592]

Berg JM, Latzman RD, Bliwise NG, & Lilienfeld SO (2015). Parsing the heterogeneity of impulsivity: A meta-analytic review of the behavioral implications of the UPPS for psychopathology. Psychological Assessment, 27(4), 1129–1146. 10.1037/pas0000111 [PubMed: 25822833]

Borne L, Rivière D, Mancip M, & Mangin J-F (2020). Automatic labeling of cortical sulci using patch- or CNN-based segmentation techniques combined with bottom-up geometric constraints. Medical Image Analysis, 62, Article 101651. 10.1016/j.media.2020.101651 [PubMed: 32163879]

Borst G, Cachia A, Tissier C, Ahr E, Simon G, & Houdé O (2016). Early cerebral constraints on reading skills in school-age children: An MRI study. Mind, Brain and Education: The Official Journal of the International Mind, Brain, and Education Society, 10(1), 47–54. 10.1111/mbe.12098

Brun L, Auzias G, Viellard M, Villeneuve N, Girard N, Poinso F, et al. (2016). Localized misfolding within Broca's area as a distinctive feature of autistic disorder. Biological Psychiatry: Cognitive Neuroscience and Neuroimaging, 1(2), 160–168. 10.1016/j.bpsc.2015.11.003 [PubMed: 29560874]

Burnham KP, & Anderson DR (2004). Multimodel inference: Understanding AIC and BIC in model selection. Sociological Methods & Research, 33(2), 261–304. 10.1177/0049124104268644

Cachia A, Borst G, Jardri R, Raznahan A, Murray GK, Mangin J-F, et al. (2021). Towards deciphering the fetal foundation of normal cognition and cognitive symptoms from sulcation of the cortex. Frontiers in Neuroanatomy, 15, Article 712862. 10.3389/fnana.2021.712862 [PubMed: 34650408]

Cachia A, Borst G, Tissier C, Fisher C, Plaze M, Gay O, et al. (2016). Longitudinal stability of the folding pattern of the anterior cingulate cortex during development. Developmental Cognitive Neuroscience, 19, 122–127. 10.1016/j.dcn.2016.02.011 [PubMed: 26974743]

Cardenas VA, Durazzo TC, Gazdzinski S, Mon A, Studholme C, & Meyerhoff DJ (2011). Brain morphology at entry into treatment for alcohol dependence is related to relapse propensity. Biological Psychiatry, 70(6), 561–567. 10.1016/j.biopsych.2011.04.003 [PubMed: 21601177]

Carver CS, & Johnson SL (2018). Impulsive reactivity to emotion and vulnerability to psychopathology. The American Psychologist, 73(9), 1067–1078. 10.1037/amp0000387 [PubMed: 30525782]

Carver CS, Johnson SL, Joormann J, Kim Y, & Nam JY (2011). Serotonin transporter polymorphism interacts with childhood adversity to predict aspects of impulsivity. Psychological Science, 22(5), 589–595. 10.1177/0956797611404085 [PubMed: 21460340]

Carver CS, Johnson SL, & Timpano KR (2017). Toward a functional view of the P factor in psychopathology. Clinical Psychological Science, 5(5), 880–889. 10.1177/2167702617710037 [PubMed: 29057170]

Carver CS, Voie LL, Kuhl J, & Ganellen RJ (1988). Cognitive concomitants of depression: A further examination of the roles of generalization, high standards, and self-criticism. Journal of Social and Clinical Psychology, 7(4), 350–365. 10.1521/jscp.1988.7.4.350

Caspi A, & Moffitt TE (2018). All for one and one for all: Mental disorders in one dimension. The American Journal of Psychiatry, 175(9), 831–844. 10.1176/appi.ajp.2018.17121383 [PubMed: 29621902]

Chakirova G, Welch KA, Moorhead TWJ, Stanfield AC, Hall J, Skehel P, et al. (2010). Orbitofrontal morphology in people at high risk of developing schizophrenia. European Psychiatry: the Journal of the Association of European Psychiatrists, 25(6), 366–372. 10.1016/j.eurpsy.2010.03.001 [PubMed: 20542665]

Chi JG, Dooling EC, & Gilles FH (1977). Gyral development of the human brain. Annals of Neurology, 1(1), 86–93. 10.1002/ana.410010109 [PubMed: 560818]

Chiavaras MM, & Petrides M (2000). Orbitofrontal sulci of the human and macaque monkey brain. The Journal of Comparative Neurology, 422(1), 35–54. https://www.ncbi.nlm.nih.gov/pubmed/10842217. [PubMed: 10842217]

Dale AM, Fischl B, & Sereno MI (1999). Cortical surface-based analysis. I. Segmentation and surface reconstruction. Neuroimage, 9(2), 179–194. 10.1006/nimg.1998.0395 [PubMed: 9931268]

Deplus S, Billieux J, Scharff C, & Philippot P (2016). A mindfulness-based group intervention for enhancing self-regulation of emotion in late childhood and adolescence: A pilot study. International Journal of Mental Health and Addiction, 14(5), 775–790. 10.1007/s11469-015-9627-1

Drevets WC (2007). Orbitofrontal cortex function and structure in depression. Annals of the New York Academy of Sciences, 1121, 499–527. 10.1196/annals.1401.029 [PubMed: 17872395]

Eckart C, Stoppel C, Kaufmann J, Tempelmann C, Hinrichs H, Elbert T, et al. (2011). Structural alterations in lateral prefrontal, parietal and posterior midline regions of men with chronic posttraumatic stress disorder. Journal of Psychiatry & Neuroscience: JPN, 36(3), 176–186. 10.1503/jpn.100010 [PubMed: 21118656]

Eichert N, Watkins KE, Mars RB, & Petrides M (2021). Morphological and functional variability in central and subcentral motor cortex of the human brain. Brain Structure & Function, 226(1), 263–279. 10.1007/s00429-020-02180-w [PubMed: 33355695]

Elliott MV, Esmail SAS, Weiner KS, & Johnson SL (2023). Neuroanatomical correlates of emotion-related impulsivity. Biological Psychiatry, 93(6), 566–574. 10.1016/j.biopsych.2022.07.018 [PubMed: 36244800]

Engvig A, Fjell AM, Westlye LT, Moberget T, Sundseth Ø, Larsen VA, et al. (2010). Effects of memory training on cortical thickness in the elderly. Neuroimage, 52(4), 1667–1676. 10.1016/j.neuroimage.2010.05.041 [PubMed: 20580844]

Fischl B, & Dale AM (2000). Measuring the thickness of the human cerebral cortex from magnetic resonance images. Proceedings of the National Academy of Sciences of the United States of America, 97(20), 11050–11055. 10.1073/pnas.200033797 [PubMed: 10984517]

Fischl B, Sereno MI, Tootell RB, & Dale AM (1999). High-resolution intersubject averaging and a coordinate system for the cortical surface. Human Brain Mapping, 8(4), 272–284. 10.1002/(sici)1097-0193(1999)8:4<272::aid-hbm10>3.0.co;2-4 [PubMed: 10619420]

Fornito A, Yücel M, Wood SJ, Proffitt T, McGorry PD, Velakoulis D, et al. (2006). Morphology of the paracingulate sulcus and executive cognition in schizophrenia. Schizophrenia Research, 88(1–3), 192–197. 10.1016/j.schres.2006.06.034 [PubMed: 16893628]

Foster BL, Koslov SR, Aponik-Gremillion L, Monko ME, Hayden BY, & Heilbronner SR (2023). A tripartite view of the posterior cingulate cortex. Nature Reviews. Neuroscience, 24(3), 173–189. 10.1038/s41583-022-00661-x [PubMed: 36456807]

Fox KCR, Nijeboer S, Dixon ML, Floman JL, Ellamil M, Rumak SP, et al. (2014). Is meditation associated with altered brain structure? A systematic review and meta-analysis of morphometric neuroimaging in meditation practitioners. Neuroscience and Biobehavioral Reviews, 43, 48–73. 10.1016/j.neubiorev.2014.03.016 [PubMed: 24705269]

Garrison JR, Fernyhough C, McCarthy-Jones S, Haggard M, Australian Schizophrenia Research Bank, Simons JS (2015). Paracingulate sulcus morphology is associated with hallucinations in the human brain. Nature Communications, 6, 8956. 10.1038/ncomms9956

Ghojogh B, & Crowley M (2019). The theory behind overfitting, cross validation, regularization, bagging, and boosting: Tutorial. arXiv preprint arXiv, 1905, 12787. http://arxiv.org/abs/1905.12787.

Gratton C, Kraus BT, Greene DJ, Gordon EM, Laumann TO, Nelson SM, et al. (2020). Defining individual-specific functional neuroanatomy for precision psychiatry. Biological Psychiatry, 88(1), 28–39. 10.1016/j.biopsych.2019.10.026 [PubMed: 31916942]

Hao L, Bao S, Tang Y, Gao R, Parvathaneni P, Miller JA, et al. (2020). Automatic labeling of cortical sulci using spherical convolutional neural networks in a developmental cohort. In 2020 IEEE 17th International Symposium on biomedical imaging (ISBI) (pp. 412–415). 10.1109/ISBI45749.2020.9098414

Hazlett EA, New AS, Newmark R, Haznedar MM, Lo JN, Speiser LJ, et al. (2005). Reduced anterior and posterior cingulate gray matter in borderline personality disorder. Biological Psychiatry, 58(8), 614–623. 10.1016/j.biopsych.2005.04.029 [PubMed: 15993861]

Heinze G, Wallisch C, & Dunkler D (2018). Variable selection - a review and recommendations for the practicing statistician. Biometrical Journal. Biometrische Zeitschrift, 60(3), 431–449. 10.1002/bimj.201700067 [PubMed: 29292533]

Hiser J, & Koenigs M (2018). The multifaceted role of the ventromedial prefrontal cortex in emotion, decision making, social cognition, and psychopathology. Biological Psychiatry, 83(8), 638–647. 10.1016/j.biopsych.2017.10.030 [PubMed: 29275839]

Hoptman MJ, Antonius D, Mauro CJ, Parker EM, & Javitt DC (2014). Cortical thinning, functional connectivity, and mood-related impulsivity in schizophrenia: Relationship to aggressive attitudes and behavior. The American Journal of Psychiatry, 171(9), 939–948. 10.1176/appi.ajp.2014.13111553 [PubMed: 25073506]

Jensen KB, Kosek E, Wicksell R, Kemani M, Olsson G, Merle JV, et al. (2012). Cognitive Behavioral Therapy increases pain-evoked activation of the prefrontal cortex in patients with fibromyalgia. Pain, 153(7), 1495–1503. 10.1016/j.pain.2012.04.010 [PubMed: 22617632]

Johnson SL, Carver CS, & Joormann J (2013). Impulsive responses to emotion as a transdiagnostic vulnerability to internalizing and externalizing symptoms. Journal of Affective Disorders, 150(3), 872–878. 10.1016/j.jad.2013.05.004 [PubMed: 23726781]

Johnson SL, Elliott MV, & Carver CS (2020). Impulsive responses to positive and negative emotions: Parallel neurocognitive correlates and their implications. Biological Psychiatry, 87(4), 338–349. 10.1016/j.biopsych.2019.08.018 [PubMed: 31668478]

Johnson SL, Tharp JA, Peckham AD, Carver CS, & Haase CM (2017). A path model of different forms of impulsivity with externalizing and internalizing psychopathology: Towards greater specificity. The British Journal of Clinical Psychology/the British Psychological Society, 56(3), 235–252. 10.1111/bjc.12135

Katzman R, Brown T, Fuld P, Peck A, Schechter R, & Schimmel H (1983). Validation of a short orientation-memory-concentration test of congestive impairment. The American Journal of Psychiatry, 140(6), 734–739. 10.1176/ajp.140.6.734 [PubMed: 6846631]

Lavoie S, Bartholomeuz CF, Nelson B, Lin A, McGorry PD, Velakoulis D, et al. (2014). Sulcogyral pattern and sulcal count of the orbitofrontal cortex in individuals at ultra high risk for psychosis. Schizophrenia Research, 154(1–3), 93–99. 10.1016/j.schres.2014.02.008 [PubMed: 24630136]

Le Provost J-B, Bartres-Faz D, Paillere-Martinot M-L, Artiges E, Pappata S, Recasens C, et al. (2003). Paracingulate sulcus morphology in men with early-onset schizophrenia. The British Journal of Psychiatry: the Journal of Mental Science, 182, 228–232. 10.1192/bjp.182.3.228 [PubMed: 12611786]

Lee S, Willbrand EH, Parker BJ, Bunge SA, Weiner KS, et al. (2024). Leveraging input-level feature deformation with guided-attention for sulcal labeling. IEEE Trans Med Imaging, 1, 1 10.1109/TMI.2024.3468727.

Leech R, & Sharp DJ (2014). The role of the posterior cingulate cortex in cognition and disease. Brain: a Journal of Neurology, 137(Pt 1), 12–32. 10.1093/brain/awt162 [PubMed: 23869106]

Leon AC, Olfson M, Portera L, Farber L, & Sheehan DV (1997). Assessing psychiatric impairment in primary care with the Sheehan Disability Scale. International Journal of Psychiatry in Medicine, 27(2), 93–105. 10.2190/T8EM-C8YH-373N-1UWD [PubMed: 9565717]

Li Y, Sescousse G, Amiez C, & Dreher J-C (2015). Local morphology predicts functional organization of experienced value signals in the human orbitofrontal cortex. The Journal of Neuroscience: the Official Journal of the Society for Neuroscience, 35(4), 1648–1658. 10.1523/JNEUROSCI.3058-14.2015 [PubMed: 25632140]

Lopez-Persem A, Verhagen L, Amiez C, Petrides M, & Sallet J (2019). The human ventromedial prefrontal cortex: Sulcal morphology and its influence on functional organization. The Journal of Neuroscience: the Official Journal of the Society for Neuroscience, 39(19), 3627–3639. 10.1523/JNEUROSCI.2060-18.2019 [PubMed: 30833514]

Maboudian SA, Willbrand EH, Kelly JP, Jagust WJ, Weiner KS, & Alzheimer's Disease Neuroimaging Initiative. (2024). Defining overlooked structures reveals new associations between the cortex and cognition in aging and Alzheimer's disease. The Journal of Neuroscience: the Official Journal of the Society for Neuroscience, 44(16). 10.1523/JNEUROSCI.1714-23.2024

Miglin R, Bounoua N, Goodling S, Sheehan A, Spielberg JM, & Sadeh N (2019). Cortical thickness links impulsive personality traits and risky behavior. Brain Sciences, 9(12). 10.3390/brainsci9120373

Miller JA, D'Esposito M, & Weiner KS (2021). Using tertiary sulci to map the "cognitive globe" of prefrontal cortex. Journal of Cognitive Neuroscience, 1–18. 10.1162/jocn_a_01696

Miller JA, Voorhies WI, Lurie DJ, D'Esposito M, & Weiner KS (2021). Overlooked tertiary sulci serve as a meso-scale link between microstructural and functional properties of human lateral prefrontal cortex. The Journal of Neuroscience: the Official Journal of the Society for Neuroscience, 41(10), 2229–2244. 10.1523/JNEUROSCI.2362-20.2021 [PubMed: 33478989]

Miotto EC, Savage CR, Evans JJ, Wilson BA, Martins MGM, Iaki S, et al. (2006). Bilateral activation of the prefrontal cortex after strategic semantic cognitive training. Human Brain Mapping, 27(4), 288–295. 10.1002/hbm.20184 [PubMed: 16082657]

Nakamura M, Nestor PG, Levitt JJ, Cohen AS, Kawashima T, Shenton ME, et al. (2008). Orbitofrontal volume deficit in schizophrenia and thought disorder. Brain: a Journal of Neurology, 131(Pt 1), 180–195. 10.1093/brain/awm265 [PubMed: 18056163]

Nakamura M, Nestor PG, McCarley RW, Levitt JJ, Hsu L, Kawashima T, et al. (2007). Altered orbitofrontal sulcogyral pattern in schizophrenia. Brain: a Journal of Neurology, 130(Pt 3), 693–707. 10.1093/brain/awm007 [PubMed: 17347256]

Nakamura M, Nestor PG, & Shenton ME (2020). Orbitofrontal sulcogyral pattern as a transdiagnostic trait marker of early neurodevelopment in the social brain. Clinical EEG and Neuroscience: Official Journal of the EEG and Clinical Neuroscience Society, 51(4), 275–284. 10.1177/1550059420904180

Nishikawa Y, Takahashi T, Takayanagi Y, Furuichi A, Kido M, Nakamura M, et al. (2016). Orbitofrontal sulcogyral pattern and olfactory sulcus depth in the schizophrenia spectrum. European Archives of Psychiatry and Clinical Neuroscience, 266(1), 15–23. 10.1007/s00406-015-0587-z [PubMed: 25757375]

Owens MM, Hyatt CS, Gray JC, Miller JD, Lynam DR, Hahn S, et al. (2020). Neuroanatomical correlates of impulsive traits in children aged 9 to 10. Journal of Abnormal Psychology, 129(8), 831–844. 10.1037/abn0000627 [PubMed: 32897083]

Parker BJ, Voorhies WI, Jiahui G, Miller JA, Willbrand E, Hallock T, et al. (2023). Hominoid-specific sulcal variability is related to face perception ability. Brain Structure & Function, 228(2), 677–685. 10.1007/s00429-023-02611-4 [PubMed: 36786881]

Patti MA, & Troiani V (2018). Orbitofrontal sulcogyral morphology is a transdiagnostic indicator of brain dysfunction. NeuroImage. Clinical, 17, 910–917. 10.1016/j.nicl.2017.12.021 [PubMed: 29527495]

Pearlstein JG, Johnson SL, Modavi K, Peckham AD, & Carver CS (2019). Neurocognitive mechanisms of emotion-related impulsivity: The role of arousal. Psychophysiology, 56(2). 10.1111/psyp.13293

Pearson CM, Combs JL, Zapolski TCB, & Smith GT (2012). A longitudinal transactional risk model for early eating disorder onset. Journal of Abnormal Psychology, 121(3), 707–718. 10.1037/a0027567 [PubMed: 22428790]

Peckham AD, & Johnson SL (2018). Cognitive control training for emotion-related impulsivity. Behaviour Research and Therapy, 105, 17–26. 10.1016/j.brat.2018.03.009 [PubMed: 29609103]

Petrides M (2019). Atlas of the morphology of the human cerebral cortex on the average MNI brain. Academic Press. https://play.google.com/store/books/details?id=qeWcBAAAQBAJ.

Poldrack RA, Huckins G, & Varoquaux G (2020). Establishment of best practices for evidence for prediction: A review: A review. JAMA Psychiatry (Chicago, Ill.), 77(5), 534–540. 10.1001/jamapsychiatry.2019.3671

Ramos Benitez J, Kannan S, Hastings WL, Parker BJ, Willbrand EH, & Weiner KS (2024). Ventral temporal and posteromedial sulcal morphology in autism spectrum disorder. Neuropsychologia, 195, Article 108786. 10.1016/j.neuropsychologia.2024.108786 [PubMed: 38181845]

Riley EN, Combs JL, Jordan CE, & Smith GT (2015). Negative urgency and Lack of perseverance: Identification of differential pathways of onset and maintenance risk in the longitudinal prediction of nonsuicidal self-injury. Behavior Therapy, 46(4), 439–448. 10.1016/j.beth.2015.03.002 [PubMed: 26163709]

Rodrigues TP, Rodrigues MAS, Paz D. de A., Costa M. D. S. da, Centeno RS, Chaddad Neto FE, et al. (2015). Orbitofrontal sulcal and gyrus pattern in human: An anatomical study. Arquivos de Neuro-Psiquiatria, 73(5), 431–435. 10.1590/0004-282X20150048 [PubMed: 26017210]

Roell M, Cachia A, Matejko AA, Houde O, Ansari D, & Borst G (2021). Sulcation of the intraparietal sulcus is related to symbolic but not non-symbolic number skills. Developmental Cognitive Neuroscience, 51, Article 100998. 10.1016/j.dcn.2021.100998 [PubMed: 34388639]

Rogers JC, & De Brito SA (2016). Cortical and subcortical gray matter volume in youths with conduct problems: A meta-analysis. JAMA Psychiatry, 73(1), 64–72. 10.1001/jamapsychiatry.2015.2423 [PubMed: 26650724]

Rolls ET (2004). The functions of the orbitofrontal cortex. Brain and Cognition, 55(1), 11–29. 10.1016/S0278-2626(03)00277-X [PubMed: 15134840]

Rolls ET, Cheng W, & Feng J (2020). The orbitofrontal cortex: Reward, emotion and depression. Brain Communications, 2(2), fcaa196. 10.1093/braincomms/fcaa196 [PubMed: 33364600]

Sanides F (1962). Besprechung. In Sanides F (Ed.), Die Architektonik des Menschlichen Stirnhirns: Zugleich eine Darstellung der Prinzipien Seiner Gestaltung als Spiegel der Stammesgeschichtlichen Differenzierung der Grosshirnrinde (pp. 176–190). Springer Berlin Heidelberg. 10.1007/978-3-642-86210-6_6.

Sanides F (1964). Structure and function of the human frontal lobe. Neuropsychologia, 2(3), 209–219. 10.1016/0028-3932(64)90005-3

Schaarschmidt F, Ritz C, & Hothorn LA (2022). The Tukey trend test: Multiplicity adjustment using multiple marginal models. Biometrics, 78(2), 789–797. 10.1111/biom.13442 [PubMed: 33559878]

Searle SR, Speed FM, & Milliken GA (1980). Population marginal means in the linear model: An alternative to least squares means. The American Statistician, 34(4), 216–221. 10.1080/00031305.1980.10483031

Smith GT, Atkinson EA, Davis HA, Riley EN, & Oltmanns JR (2020). The general factor of psychopathology. Annual Review of Clinical Psychology, 16, 75–98. 10.1146/annurev-clinpsy-071119-115848

Takahashi T, Nakamura Y, Nakamura K, Ikeda E, Furuichi A, Kido M, et al. (2013). Altered depth of the olfactory sulcus in first-episode schizophrenia. Progress in Neuro-Psychopharmacology & Biological Psychiatry, 40, 167–172. 10.1016/j.pnpbp.2012.10.001 [PubMed: 23063493]

Takahashi T, Nakamura M, Sasabayashi D, Nishikawa Y, Takayanagi Y, Furuichi A, et al. (2019). Association between olfactory sulcus morphology and olfactory functioning in schizophrenia and psychosis high-risk status. Heliyon, 5(10), Article e02642. 10.1016/j.heliyon.2019.e02642 [PubMed: 31667432]

Takahashi T, Wood SJ, Yung AR, Nelson B, Lin A, Yücel M, et al. (2014). Altered depth of the olfactory sulcus in ultra high-risk individuals and patients with psychotic disorders. Schizophrenia Research, 153(1–3), 18–24. 10.1016/j.schres.2014.01.041 [PubMed: 24530137]

Troiani V, Dougherty CC, Michael AM, & Olson IR (2016). Characterization of face-selective patches in orbitofrontal cortex. Frontiers in Human Neuroscience, 10, 279. 10.3389/fnhum.2016.00279 [PubMed: 27378880]

Troiani V, Patti MA, & Adamson K (2020). The use of the orbitofrontal H-sulcus as a reference frame for value signals. The European Journal of Neuroscience, 51(9), 1928–1943. 10.1111/ejn.14590 [PubMed: 31605399]

Turetsky BI, Crutchley P, Walker J, Gur RE, & Moberg PJ (2009). Depth of the olfactory sulcus: A marker of early embryonic disruption in schizophrenia? Schizophrenia Research, 115(1), 8–11. 10.1016/j.schres.2009.09.005 [PubMed: 19767178]

Uehara-Aoyama K, Nakamura M, Asami T, Yoshida T, Hayano F, Roppongi T, et al. (2011). Sexually dimorphic distribution of orbitofrontal sulcogyral pattern in schizophrenia. Psychiatry and Clinical Neurosciences, 65(5), 483–489. 10.1111/j.1440-1819.2011.02229.x [PubMed: 21851457]

Vabalas A, Gowen E, Poliakoff E, & Casson AJ (2019). Machine learning algorithm validation with a limited sample size. Plos One, 14(11), Article e0224365. 10.1371/journal.pone.0224365 [PubMed: 31697686]

Voorhies WI, Miller JA, Yao JK, Bunge SA, & Weiner KS (2021). Cognitive insights from tertiary sulci in prefrontal cortex. Nature Communications, 12(1), 5122. 10.1038/s41467-021-25162-w

Wagenmakers E-J, & Farrell S (2004). AIC model selection using Akaike weights. Psychonomic Bulletin & Review, 11(1), 192–196. 10.3758/bf03206482 [PubMed: 15117008]

Wandell BA, Chial S, & Backus BT (2000). Visualization and measurement of the cortical surface. Journal of Cognitive Neuroscience, 12(5), 739–752. 10.1162/089892900562561 [PubMed: 11054917]

Watanabe H, Nakamura M, Ohno T, Itahashi T, Tanaka E, Ohta H, et al. (2014). Altered orbitofrontal sulcogyral patterns in adult males with high-functioning autism spectrum disorders. Social Cognitive and Affective Neuroscience, 9(4), 520–528. 10.1093/scan/nst016 [PubMed: 23386741]

Welker W (1990). Why does cerebral cortex fissure and fold? In Jones EG, & Peters A (Eds.), Cerebral cortex: Comparative structure and evolution of cerebral cortex, Part II (pp. 3–136). Springer US. 10.1007/978-1-4615-3824-0_1.

Whiteside SP, & Lynam DR (2001). The five factor model and impulsivity: Using a structural model of personality to understand impulsivity. Personality and Individual Differences, 30(4), 669–689. 10.1016/S0191-8869(00)00064-7

Whittle S, Bartholomeusz C, Yücel M, Dennison M, Vijayakumar N, & Allen NB (2014). Orbitofrontal sulcogyral patterns are related to temperamental risk for psychopathology. Social Cognitive and Affective Neuroscience, 9(2), 232–239. 10.1093/scan/nss126 [PubMed: 23160816]

Willbrand EH, Ferrer E, Bunge SA, & Weiner KS (2023). Development of human lateral prefrontal sulcal morphology and its relation to reasoning performance. The Journal of Neuroscience: the Official Journal of the Society for Neuroscience, 43(14), 2552–2567. 10.1523/JNEUROSCI.1745-22.2023 [PubMed: 36828638]

Willbrand EH, Jackson S, Chen S, Hathaway CB, Voorhies WI, Bunge SA, et al. (2024). Sulcal variability in anterior lateral prefrontal cortex contributes to variability in reasoning performance among young adults. Brain Structure & Function. 10.1007/s00429-023-02734-8

Willbrand EH, Maboudian SA, Kelly JP, Parker BJ, Foster BL, & Weiner KS (2023). Sulcal morphology of posteromedial cortex substantially differs between humans and chimpanzees. Communications Biology, 6(1), 1–14. 10.1038/s42003-023-04953-5 [PubMed: 36596887]

Willbrand EH, Parker BJ, Voorhies WI, Miller JA, Lyu I, Hallock T, et al. (2022). Uncovering a tripartite landmark in posterior cingulate cortex. Science Advances, 8(36), Article eabn9516. 10.1126/sciadv.abn9516 [PubMed: 36070384]

Willbrand EH, Tsai Y-H, Gagnant T, & Weiner KS (2023). Updating the sulcal landscape of the human lateral parieto-occipital junction provides anatomical, functional, and cognitive insights. eLife. 10.7554/elife.90451.1

Willbrand EH, Voorhies WI, Yao JK, Weiner KS, & Bunge SA (2022). Presence or absence of a prefrontal sulcus is linked to reasoning performance during child development. Brain Structure & Function, 227(7), 2543–2551. 10.1007/s00429-022-02539-1 [PubMed: 35932310]

Yücel M, Stuart GW, Maruff P, Wood SJ, Savage GR, Smith DJ, et al. (2002). Paracingulate morphologic differences in males with established schizophrenia: A magnetic resonance imaging morphometric study. Biological Psychiatry, 52(1), 15–23. 10.1016/s0006-3223(02)01312-4 [PubMed: 12079726]

Yao JK, Voorhies WI, Miller JA, Bunge SA, & Weiner KS (2022). Sulcal depth in prefrontal cortex: A novel predictor of working memory performance. Cerebral Cortex. 10.1093/cercor/bhac173. bhac173.

Yarkoni T, Poldrack RA, Nichols TE, Van Essen DC, & Wager TD (2011). Large-scale automated synthesis of human functional neuroimaging data. Nature Methods, 8(8), 665–670. 10.1038/nmeth.1635 [PubMed: 21706013]

Zachlod D, Palomero-Gallagher N, Dickscheid T, & Amunts K (2023). Mapping cytoarchitectonics and receptor architectonics to understand brain function and connectivity. Biological Psychiatry, 93(5), 471–479. 10.1016/j.biopsych.2022.09.014 [PubMed: 36567226]

Zeidan F, Emerson NM, Farris SR, Ray JN, Jung Y, McHaffie JG, et al. (2015). Mindfulness meditation-based pain relief employs different neural mechanisms than placebo and sham mindfulness meditation-induced analgesia. The Journal of Neuroscience: the Official Journal of the Society for Neuroscience, 35(46), 15307–15325. 10.1523/JNEUROSCI.2542-15.2015 [PubMed: 26586819]

Zhao J, Tomasi D, Wiers CE, Shokri-Kojori E, Demiral ŞB, Zhang Y, et al. (2017). Correlation between traits of emotion-based impulsivity and intrinsic default-mode network activity. Neural Plasticity, 2017, Article 9297621. 10.1155/2017/9297621 [PubMed: 29225975]

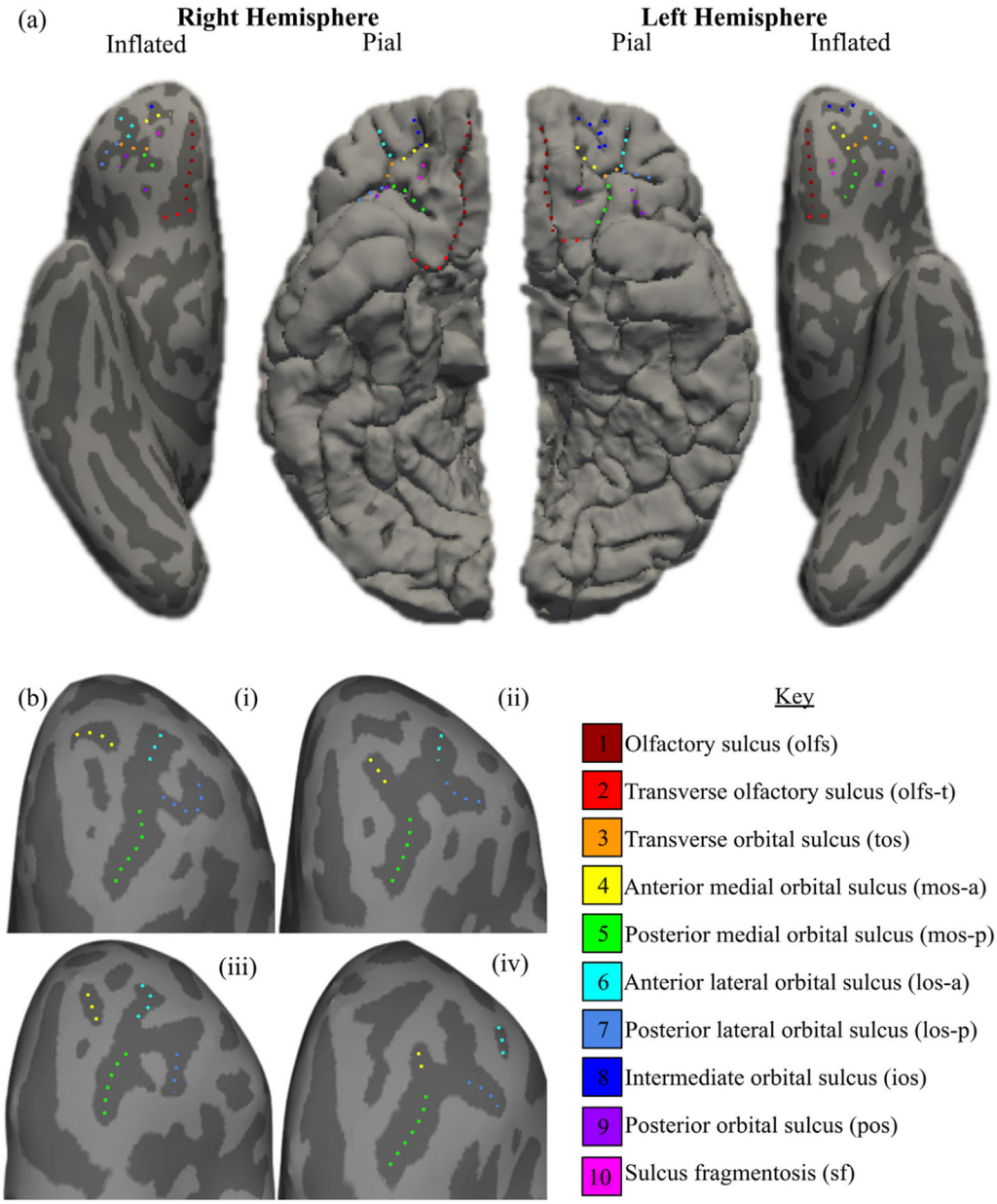

Fig. 1 –.

Sulci and sulcogyral types in orbitofrontal cortex. (a) OFC sulcogyral organization labeled on pial (middle surfaces) and inflated (outer surfaces) surfaces in the left (right surfaces) and right (left surfaces) hemispheres. On these cortical reconstructions, sulci are dark gray and gyri are light gray. Sulci are outlined according to the key beside b. Sulci are labeled according to a revised version of Petrides' (2019) atlas. Example hemispheres shown have all variable sulci, which is not always the case with participants in this study. See Supplementary Fig. 1 for OFC sulcal definitions in all hemispheres. (b) Examples of the different OFC patterns as defined by Chiavaras and Petrides (2000) and refined by Chakirova et al. (2010).

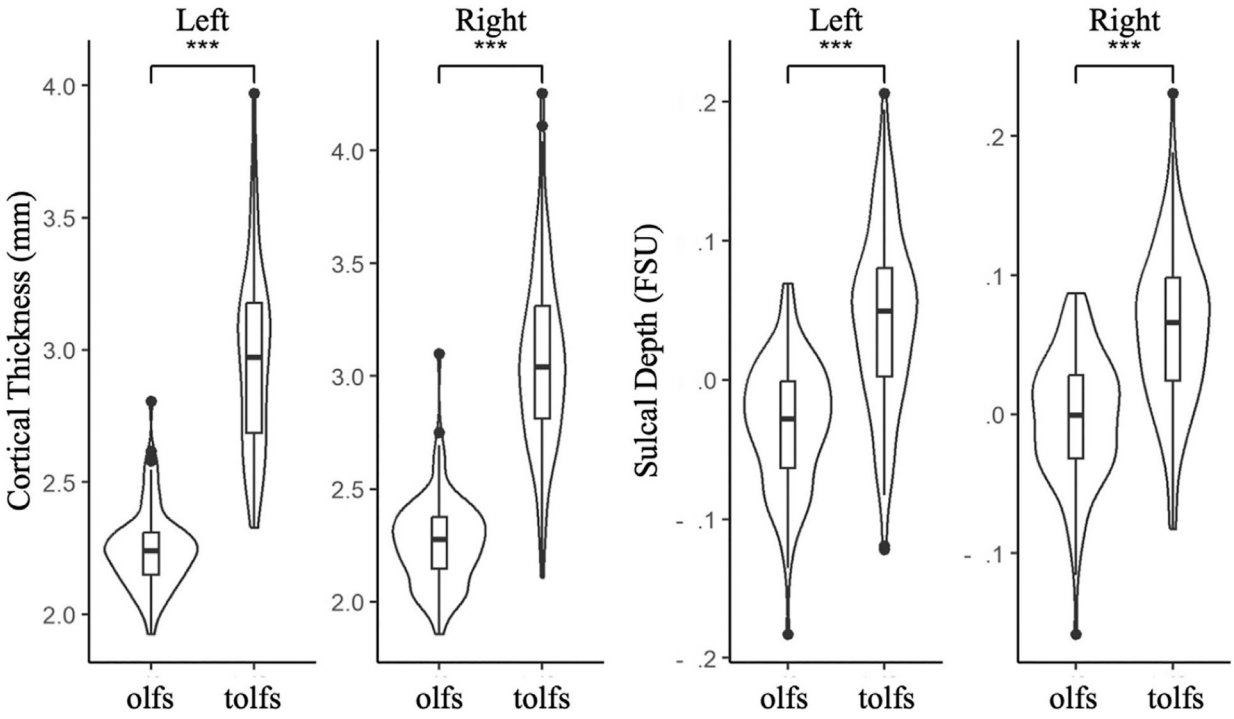

Fig. 2 –.

The transverse olfactory sulcus is cortically thicker and deeper than the olfactory sulcus. Distributions are represented by box plots. Outliers are represented as points. Significant differences are denoted by bars above the graph. Cortical thickness is measured in millimeters (mm) and sulcal depth is measured in FreeSurfer Units (FSU; Materials and Methods). Sulcal abbreviations correspond to those used in Fig. 1. The cortical thickness and sulcal depth of all OFC sulci are shown in Supplementary Fig. 3. ***$P < .0001$.

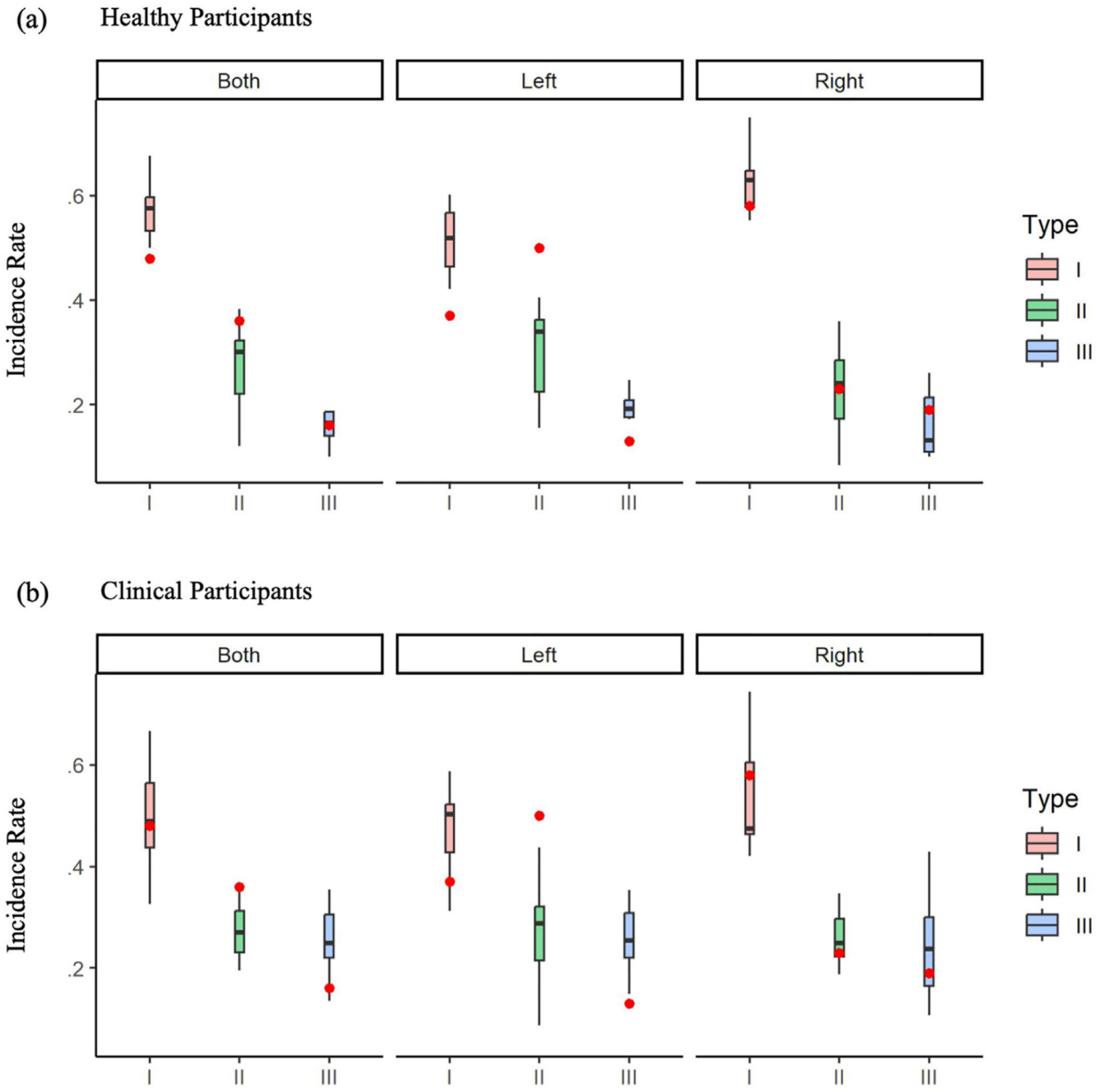

Fig. 3 –.

OFC sulcogyral types in the present study are consistent with a meta-analysis of the previous OFC literature. Red points represent the incidence rate observed in this sample in comparison to boxplots of incidence rates observed across several studies in both hemispheres as well as left and right hemispheres individually in (a) healthy (12 studies, 710 total participants), and (b) clinical samples (13 studies, 869 total participants). Type IV was excluded due to inconsistent inclusion across the literature.

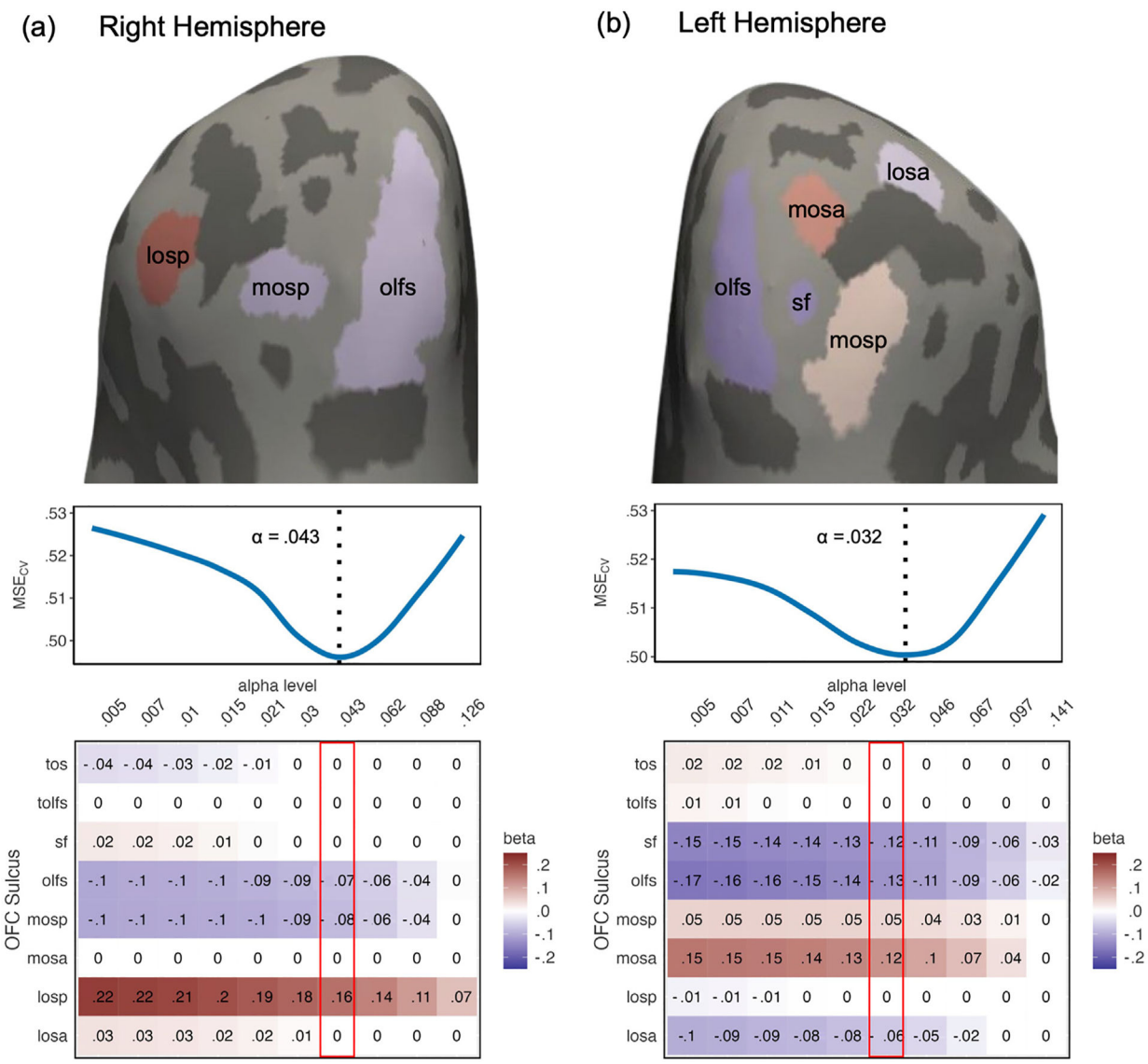

Fig. 4 –.

Data-driven model selection reveals a relationship between OFC sulcal depth and emotion-related impulsivity. Inflated cortical surfaces including LASSO selected sulci (top) colored according to the beta values (bottom) in the right (a) and left (b) hemispheres. Line graphs depict MSE at each corresponding alpha (middle). The dotted line represents the alpha which minimizes MSE. Matrices reflect the beta values of the predictors at each corresponding alpha value (bottom). Beta values used in the model which minimize MSE are outlined in red. Sulcal abbreviations correspond to those used in Fig. 1a.